a

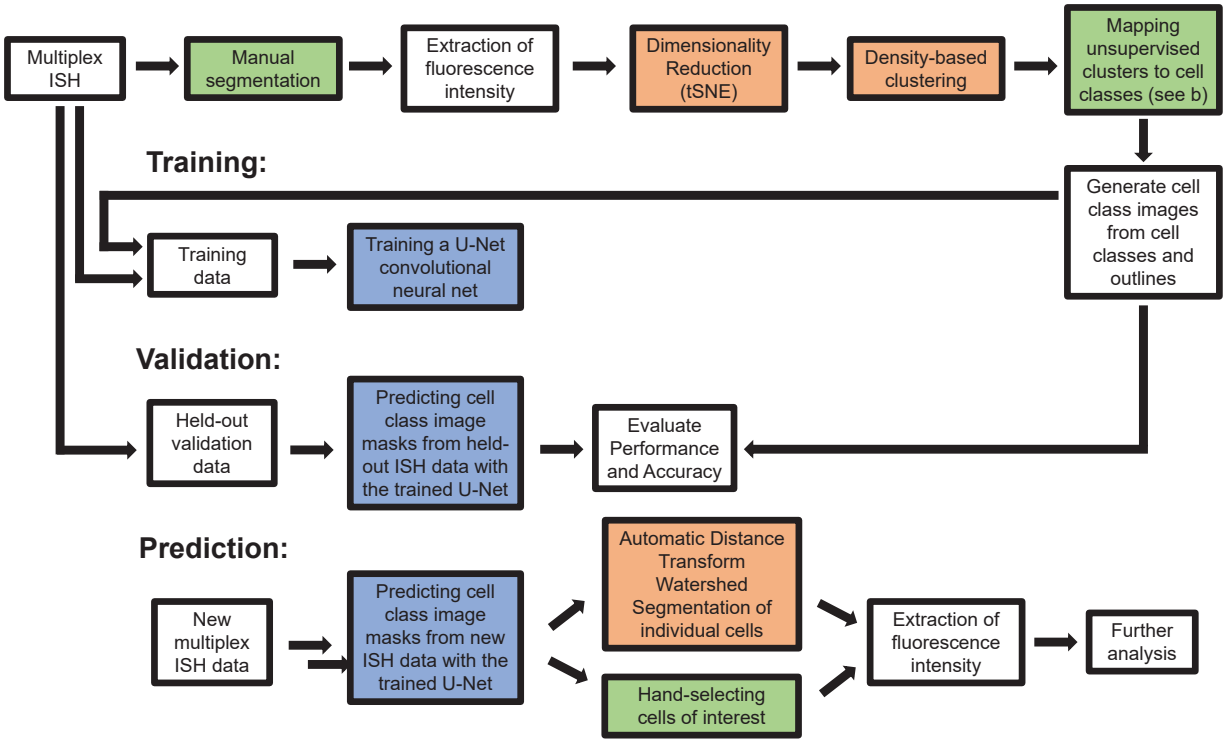

b

Cell class	Criteria for cluster mapping	Expression pattern within 8 probe model
C1	High *Trpm8*	*Trpm8* +
C3	High *Cd34*	*Fxyd2* +, *Tmem233* -, *S100b* -, *Nppb* -, *Mrgprd* -
C4	High *S100b*, low *Fxyd2*, low *Calca*	*S100b* +, *Fxyd2* -, *Calca* -
C5	High *S100b*, high *Fxyd2*	*S100b* +, *Fxyd2* +
C6	High *S100b*, high *Calca*	*S100b* +, *Calca* +
C7/9/10	High *Trpv1*, low *Trpa1*	*Calca* +, *S100b* -, *Tmem233* -, *Trpa1* -, *Fxyd2* -, *Nppb* -
C8	High *Trpa1*	*Trpa1* +, *Calca* +, *Tmem233* -, *Fxyd2*-, *Mrgprd* -
C11	High *Nppb*	*Nppb* +
C12	High *Etv1*, low *Nppb*	*Tmem233* +, *Mrgprd* -, *Nppb* -, *S100b* -
C13	High *Mrgprd*	*Mrgprd* +

Supplementary Figure 1. Data flow in the semi-supervised machine learning approach

(a) Manually generated, supervised aspects (green) and automatically generated, unsupervised aspects (brown) of the data were used to train the core U-Net Deep Learning model (blue). This model was then validated on a held-out validation data set and ultimately was used to predict cell class images from new multiplex ISH data. (b) Criteria used for cluster / cell class matching and expression patterns observed within the 8-probe model.

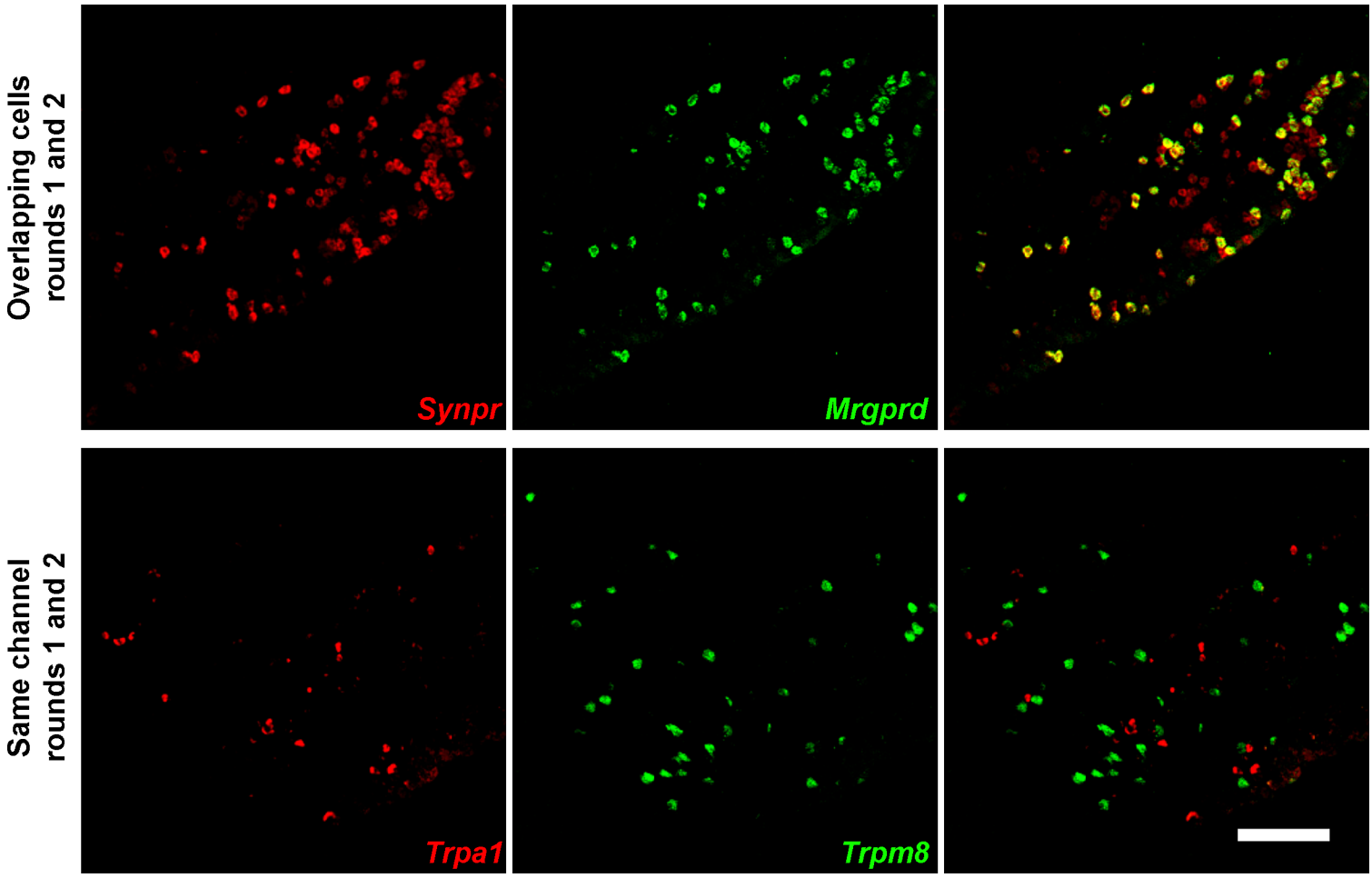

Supplementary Figure 2. Controls for multiplex ISH

Example images from different rounds of ISH on a single section. Top panels: control to show that images can be accurately aligned between rounds using rotation and transposition. A subset of cells labeled in round 1 by *Synpr* were also detected in round 2 using a probe to *Mrgprd*. These cells align perfectly as shown in the combined image. Lower panels: control to demonstrate that stripping probes prevents signal carry over between rounds. *Trpa1* and *Trpm8* are expressed in non-overlapping populations of cells and were detected using the same amplifiers and fluorophores in rounds 1 and 2 respectively. The combined image shows that these two probes detect completely non-overlapping cells confirming that there is no carryover of signal between rounds; scale bar, 100 μm.

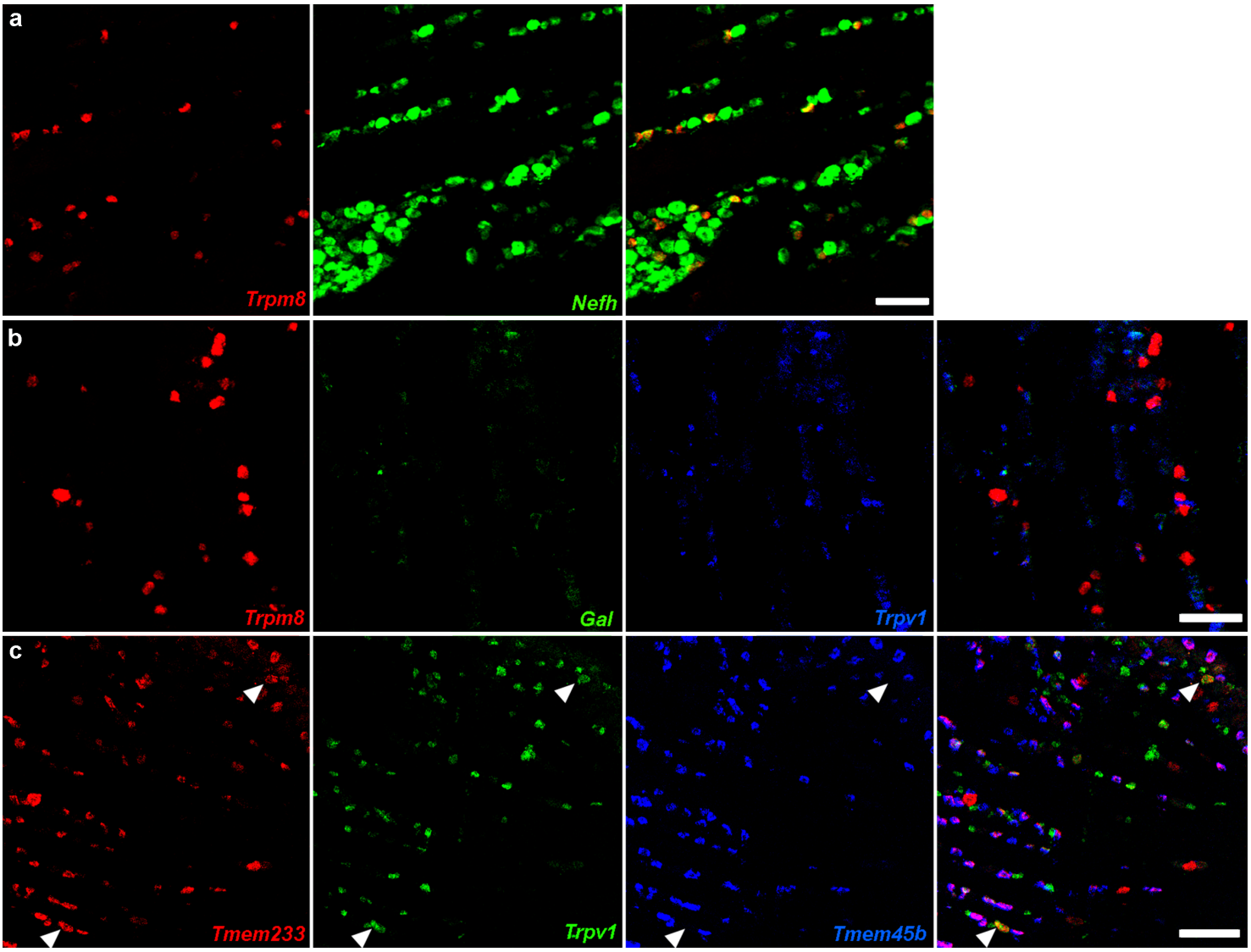

Supplementary Figure 3. Not all predicted neural classes were detected by multiplex ISH

(a) Expression of *Nefh* was predicted to divide *Trpm8* expressing neurons into 2 distinct classes (C1 and C2). However, ISH revealed that all *Trpm8* neurons expressed similar levels of *Nefh*. (b) A second marker predicted to distinguish C1 and C2 neurons was the neuropeptide galanin. ISH revealed low level expression of *Gal* in the ganglion and co-expression with *Trpv1*, rather than *Trpm8* (a marker of C1/2 neurons). Together these data suggest that the division of C1 and C2 classes in the sc-analysis may be a consequence of methodology rather than biology. (c) Single cell data divided *Trpv1*-expressing neurons into several classes. One of these, C7, was distinguished from other classes of *Trpv1* neurons by its co-expression of *Tmem233* but not *Tmem45b*. As illustrated in an example image of multiplexed ISH, a few such cells (arrowheads) could be distinguished but they failed to segregate from classes C9 and C10 in tSNE based cluster analysis (Fig. 3); scale bars, 125 μm.

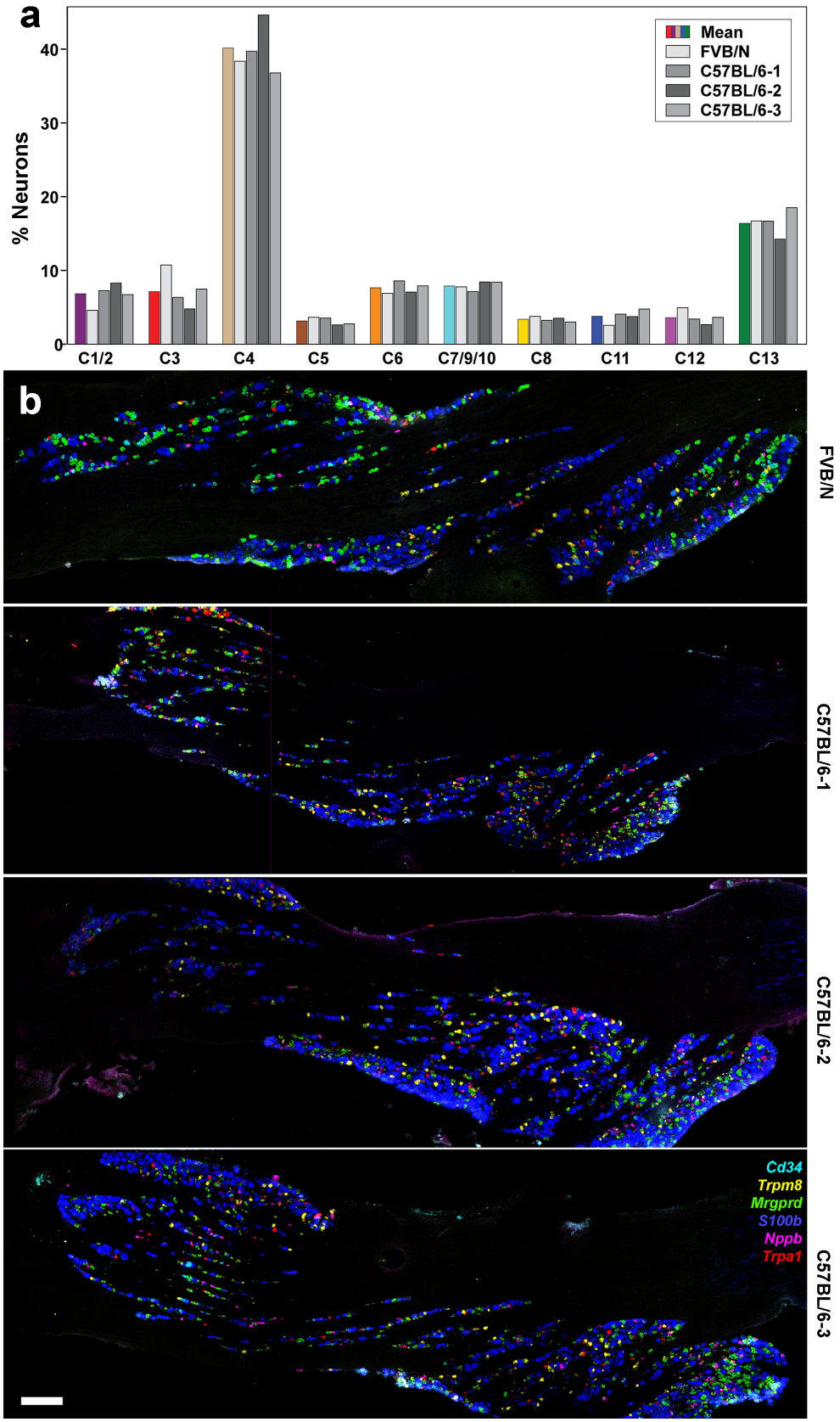

Supplementary Figure 4. High consistency in class assignment between animals and sections

(a) Bar graph showing the classification of trigeminal neurons using multiplex ISH in four animals (grey bars) and the mean values (colored bars). (b) Sections of the trigeminal ganglion from the FVB/N and three C57BL/6 mice; shown are the overlaid ISH images of 6 non-overlapping probes colored as indicated; scale bar, 200 µm.

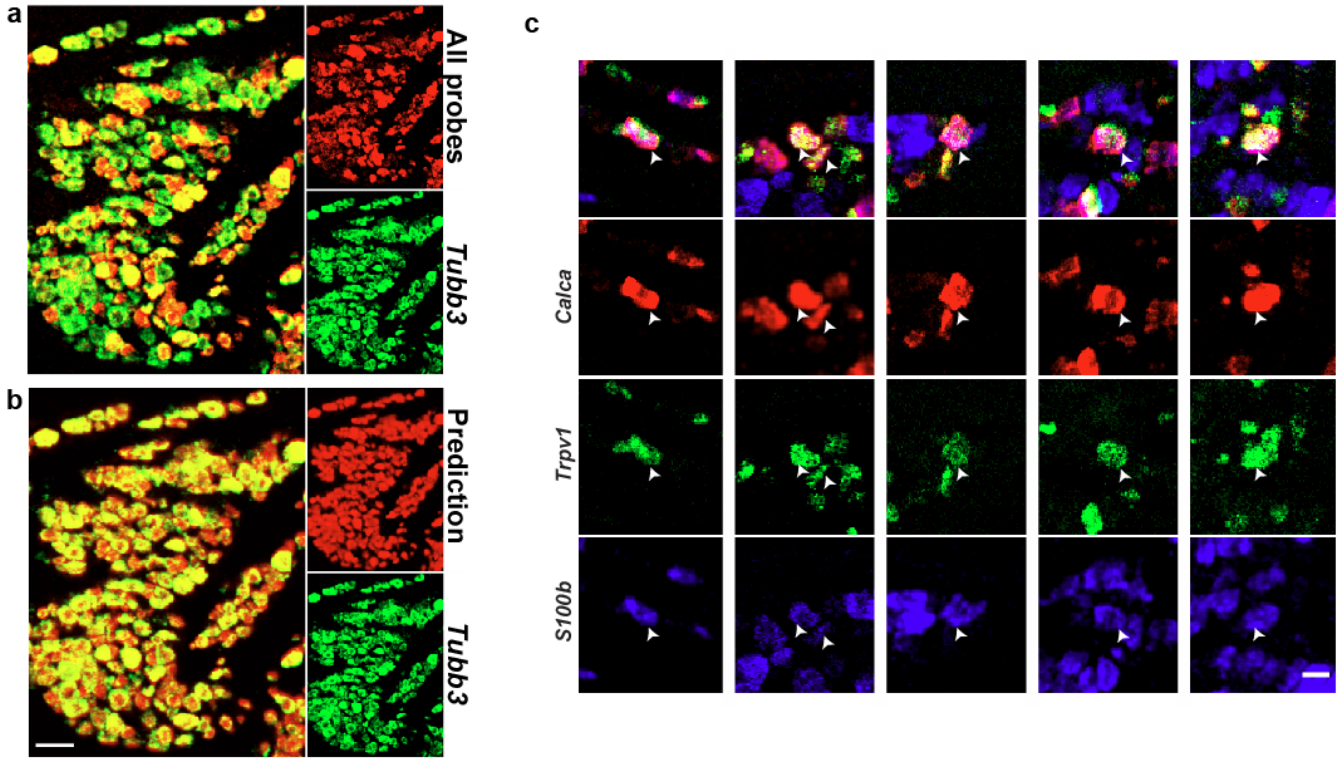

Supplementary Figure 5. ISH probes and U-Net predictions identify all trigeminal neurons

(a) Representative image showing that in combination the 13 ISH probes used in clustering-based classification of trigeminal neurons (colored red) detected all the neurons identified using a pan-neuronal *Tubb3* probe (green) and did not identify non-neuronal cells. Similarly, (b) the U-Net prediction (red) very closely matched the distribution of neurons revealed by *Tubb3* ISH (green). Importantly, predicted neurons were always *Tubb3* positive. Also note the more uniform definition of cell boundaries that can be discerned in the prediction data than in the ISH images; scale bar 100 μm. (c) Sample images selected to show a subset of C6 neurons defined by co-expression of *Calca* (red) and *S100b* (blue) also express the heat and capsaicin sensitive ion channel *Trpv1* (green); these neurons are arrowed, scale bar 20 μm.

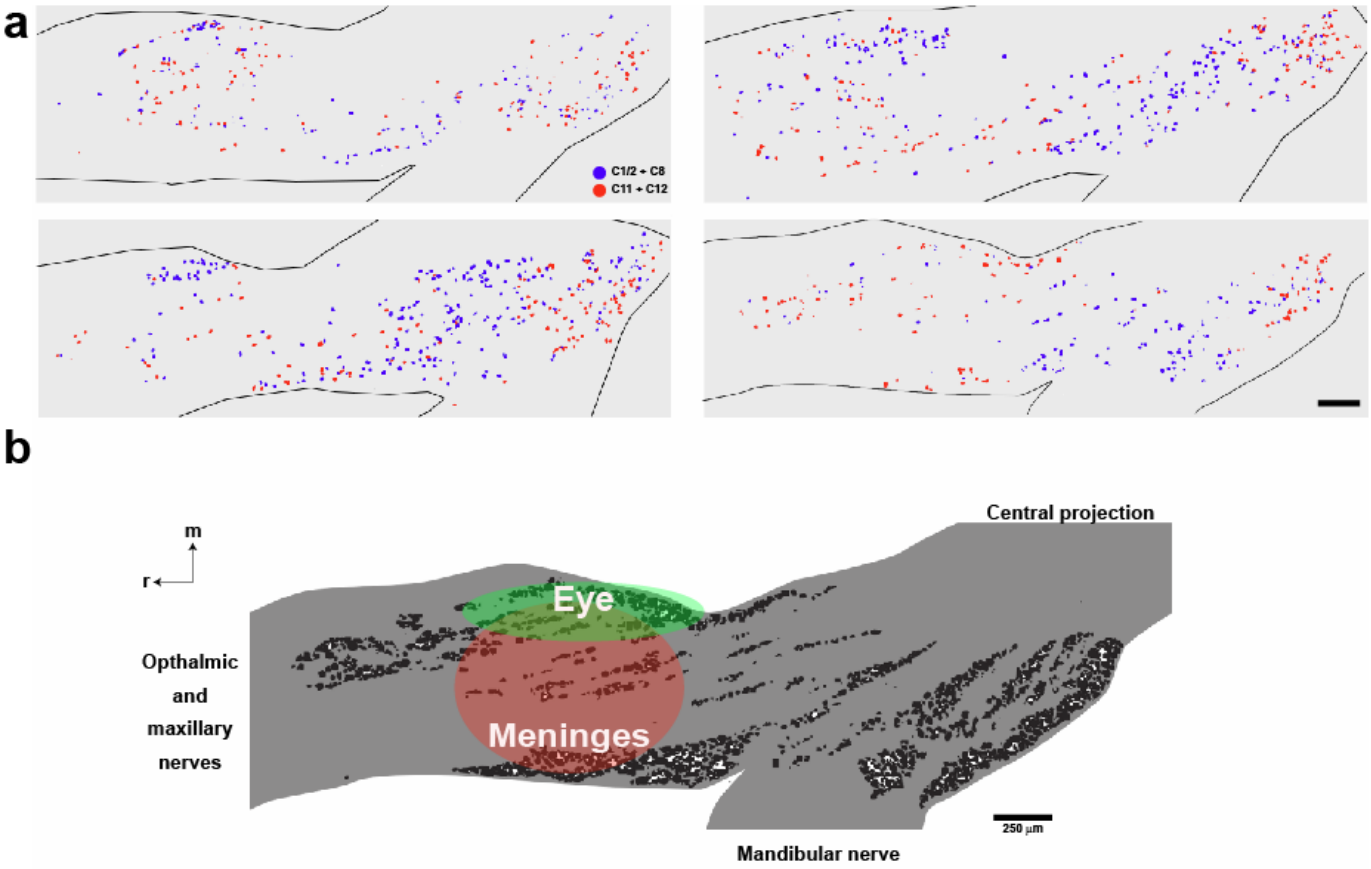

Supplementary Figure 6. Regional segregation of neural class in the trigeminal ganglion

(a) Anatomical mapping of C1/2 plus C8 neurons (blue) and C11 plus C12 neurons (red) in the sections through the trigeminal ganglion of four mice reveals extensive spatial segregation of these neural classes; differences between the four ganglia likely reflect the sectioning plane but may also include animal to animal variation. (b) WGA-labeling from the eye and meninges labeled distinctive regions of the ganglion (indicated by green and red shading); scale bars, 250 µm; m, medial; r, rostral.

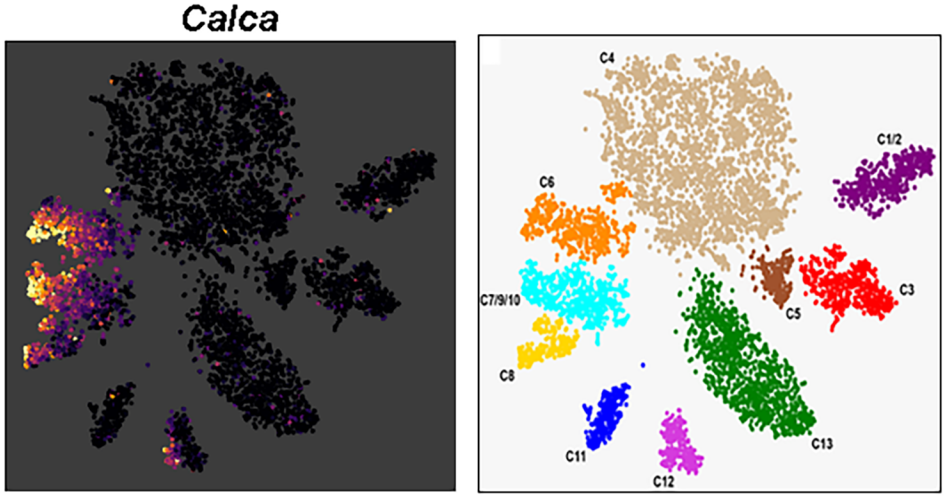

Supplementary Figure 7. tSNE representations of ISH intensities of Calca expression in trigeminal ganglion neurons

(Left panel) Cells were manually segmented and the cellular ISH intensity of *Calca* expression was assessed (see Fig. 2b). The tSNE representation highlights differences in expression between classes and shows that a fraction of C12 neurons express this gene. (Right panel) The distribution of neuronal classes is shown for comparison purposes.

Table S1 Statistical analysis of data in Fig. 5c

208 trigeminal neurons innervating the eye and 239 targeting the meninges were classified. The proportional representations of the different neuronal classes in these populations were compared with their prevalence in the trigeminal ganglion using an unpooled two-tailed z-test for proportions that does not assume common variance between the two populations. The p-values are reported for each class. In addition, where differences were significant, $p < 0.05$, the color coding indicates upregulation (pink) or downregulation (pale blue) in the neurons innervating the target.

Neuronal Class	**Eye (p-value)**	**Meninges (p-value)**
C1/2	8.65×10^{-6}	4.08×10^{-7}
C3	8.45×10^{-11}	8.19×10^{-9}
C4	5.41×10^{-8}	4.29×10^{-4}
C5	4.01×10^{-3}	0.381
C6	0.015	4.21×10^{-7}
C7/9/10	0.260	5.53×10^{-5}
C8	3.51×10^{-14}	$< 1 \times 10^{-20}$
C11	$< 1 \times 10^{-20}$	0.062
C12	0.215	7.16×10^{-5}
C13	9.37×10^{-8}	6.66×10^{-16}